Sleep and Breathing (2020) 24:287–296
https://doi.org/10.1007/s11325-019-01948-7

ENT • ORIGINAL ARTICLE

How does distraction osteogenesis maxillary expansion (DOME) reduce severity of obstructive sleep apnea?

Tomonori Iwasaki[1] · Audrey Yoon[2] · Christian Guilleminault[3] · Youichi Yamasaki[1] · Stanley Yung Liu[4]

Received: 27 December 2018 / Revised: 30 August 2019 / Accepted: 18 September 2019 / Published online: 10 December 2019

Abstract

Objective Distraction osteogenesis maxillary expansion (DOME) is a reliable method to expand the nasal floor and hard palatal vault in adults with obstructive sleep apnea (OSA). DOME results in a reduction in the apnea-hypopnea index (AHI) and subjective report of improved nasal breathing. Using rhinomanometry augmented computational fluid dynamic (CFD) modeling, we propose a mechanism of how DOME reduces upper airway pharyngeal collapse in adults with OSA.

Material and method A retrospective cohort with 20 subjects and mean age of 29.6 ± 8 years who completed DOME at Stanford University from September 2014 to April 2016. Subjects were included if polysomnography, airway morphology, and rhinomanometry were available for use. From the CBCT data, 3D nasal and pharyngeal airway model were generated. Numeric CFD simulation of the airway models were analyzed under the following conditions: (1) the volume of air was flowing at a velocity of 300 cm^3/s, (2) the wall surface was not slippery, and (3) the simulations were repeated 1000 times to calculate mean values. Statistical analyses using SPSS v24 software included paired *t* tests, nonparametric Wilcoxon rank test, Friedman test with Bonferroni correction, and Spearman's correlation coefficients ($p < 0.05$).

Results Mean AHI improved from 17.8 ± 17.6 to 7.8 ± 7.1 events per hour ($p < 0.001$). Mean lowest oxygen saturation improved from 88.2 ± 7.2 to 90.9 ± 4.2% ($p < 0.05$). Mean airflow velocity within the nasal airway decreased from 15.6 ± 7.3 to 7.4 ± 2.1 m/s ($p < 0.001$) after DOME. Mean negative pressure of the nasal airway, retropalatal airway, oropharyngeal airway, and hypopharyngeal airway is reduced from − 158.4 ± 115.3 to − 48.6 ± 28.7 Pa, from − 174.8 ± 119.9 to − 52.5 ± 31.3 Pa, from − 177.0 ± 118.4 to − 54.9 ± 31.8 Pa and from − 177.9 ± 117.9 to − 56.9 ± 32.1 Pa ($p < 0.001$), respectively. AHI positively correlated with nasal flow velocity ($p < 0.05$) and negatively correlated with pharyngeal airway pressure ($p < 0.05$). ODI was positively correlated with nasal velocity ($p < 0.05$) and negatively correlated with nasal airway pressure ($p < 0.05$), retropalatal airway pressure ($p < 0.001$), oropharyngeal airway pressure ($p < 0.001$), and hypopharyngeal airway pressure ($p < 0.05$).

Conclusion Anatomic expansion of the nasal floor with widening of the hard palatal vault from DOME is associated with reduction of nasal airflow velocity and downstream reduction of negative pressure in the pharyngeal airway. This dynamic interaction correlates with a reduction in the apnea-hypopnea index (AHI) and Oxygen Desaturation Index (ODI).

✉ Stanley Yung Liu
ycliu@stanford.edu

[1] Pediatric Dentistry, Graduate School of Medical and Dental Sciences, Kagoshima University, Kogoshima, Japan

[2] Sections of Pediatric Dentistry and Orthodontics, Division of Growth and Developments, UCLA School of Dentistry, Los Angeles, CA 90095, USA

[3] Sleep Medicine Division, Department of Psychiatry, Stanford Health Care, Redwood City, CA 94063, USA

[4] Division of Sleep Surgery, Department of Otolaryngology-Head & Neck Surgery, School of Medicine, Stanford University, 801 Welch Road, Stanford, CA 94304, USA

Keywords Distraction osteogenesis maxillary expansion · DOME · Computational fluid dynamic · Nasal airflow velocity · Pharyngeal negative pressure · Adult maxillary expansion · Sleep apnea · OSA · Nasal obstruction · Rhinomanometry · Snoring · Nasal obstruction

Introduction

Obstructive sleep apnea (OSA) is a public health concern associated with behavioral and cognitive dysfunction, cardiovascular risk, and a negative impact on the quality of life [1]. Maxillofacial hypoplasia is a predisposing factor for the development of OSA. A well-known phenotype with transverse maxillary constriction is associated with alteration in tongue posture and high nasal airway resistance [2]. Children with this phenotype have shown OSA treatment success with rapid maxillary expansion (RME) after tonsillectomy and adenoidectomy. Results are limited for adults with a similar phenotype, as techniques for maxillary expansion in adults were previously unreliable [3–7].

With the introduction of mini-implants for the facial bone, we reported Distraction osteogenesis maxillary expansion (DOME) technique to expand the adult maxilla that is similar to pediatric RME [8]. DOME was designed to address the need to expand the adult maxilla rapidly using mini-implant–assisted expander and less invasive osteotomy. DOME changes the palatal vault morphology from a narrow, high-arched shape to a dome shape with increased intraoral volume for the tongue and improved subjective nasal breathing [8, 9].

While transverse maxillary expansion increases nasal cavity volume and decreases nasal airway resistance [4], how this translates to improvement in OSA severity is unknown. We applied computational fluid dynamics (CFD) based on physiologic measurements from rhinomanometry [10, 11] to construct a dynamic airway model involving both the nasal and pharyngeal airways. We hypothesized that a reduction in nasal airflow velocity from DOME results in decreased negative pressure of the pharyngeal airway, leading to less upper airway collapsibility.

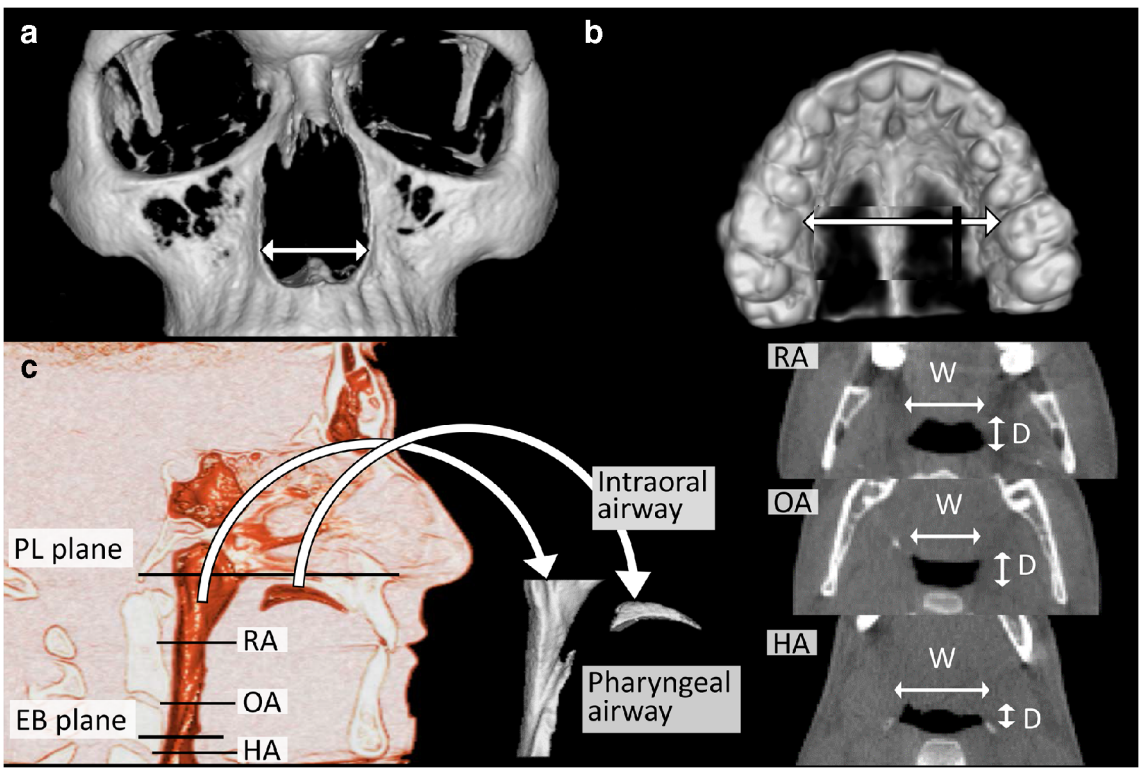

Fig. 1 Measurement of anatomical structure and airway. **A**, nasal width: the widest distance of the nasal aperture. **B**, intermaxillary molar width: the distance between the narrowest points of the first maxillary molars. **C**, Measurement of cross-sections and volumes of the airway: PL plane, a plane passing through the hard plate; EB plane, a plane parallel to the hard plate passing through the base of the epiglottis; RA, retropalatal airway, narrowest cross section was measured parallel to the PL plane; OA, oropharyngeal airway, cross section was measured parallel to the PL plane passing through the anterior-inferior corner of second vertebra; HA, hypopharyngeal airway, cross section was measured along the PL plane passing through the anterior–inferior corner of third vertebra; intraoral airway, airway between the palate and the tongue; pharyngeal airway, airway between the PL and EB planes; D, depth; W, width

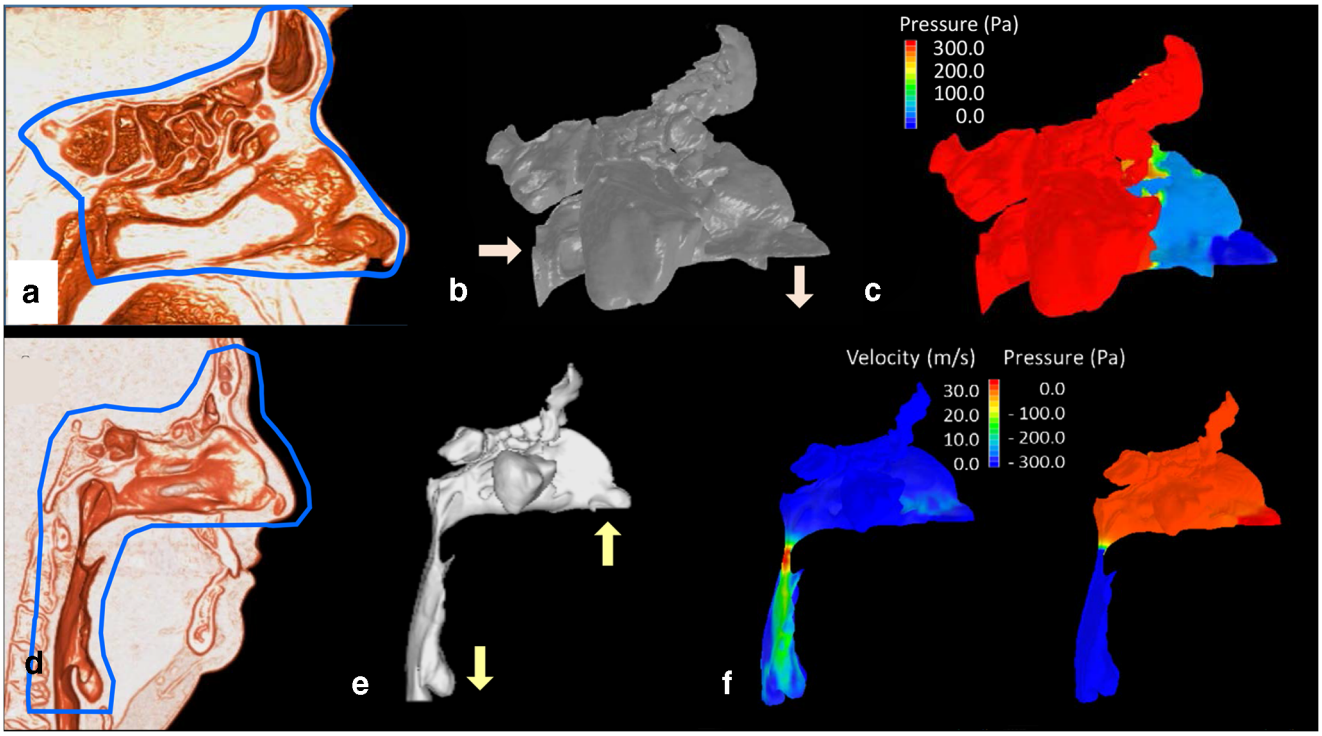

Fig. 2 Evaluation of the nasal airway model and upper airway pressures during inspiration using computational fluid dynamics. **A**, Extraction of the nasal airway. **B**, Construction of the 3D nasal airway model and numeric simulation (expiration air, light yellow arrow). **C**, Evaluation of pressure of nasal airway. The nasal resistance was calculated by dividing the pressure of the nasal airway by air flow volume. The threshold of the air in the nasal cavity model found that nasal cavity resistance value obtained in CFD corresponded to the nasal cavity resistance value of rhinomanometry that was regulated. **D**, Extraction of the upper airway. **E**, Construction of the 3D upper airway model and numeric simulation (Inspiration air, light yellow arrow). **F**, Evaluation of ventilation condition of upper airway at inspiration (left; velocity, right; pressure)

Material and methods

Design

We conducted a retrospective cohort study of 20 subjects who underwent DOME from September 2014 to April 2016.

Subjects

Subjects were adults with a diagnosis of OSA based on attended polysomnography, who were intolerant of continuous positive airway pressure (CPAP) or oral appliance therapy. They present with a narrow hard palatal roof, Mallampati class 4 (70%) or 3 (30%), and no palatine or lingual tonsillar hypertrophy. Subjects included must also have nasal rhinomanometry and cone beam computed tomography (CBCT) data available.

Polysomnography

Subjects underwent attended polysomnography (PSG) conducted and scored according to the standards of the American Academy of Sleep Medicine, including electroencephalography, electro-oculography, chin electromyography, and electrocardiography [12]. Subjects had transcutaneous pulse oximetry, with respiratory effort recorded using inductance plethysmography. Apnea was defined by decrease of baseline airflow by more than 90% for at least 10 s as measured by nasal cannula and mouth thermistor. Hypopnea was measured using a nasal pressure cannula and was defined as a partial obstructive event with decrease of airflow by 30% from baseline for at least 10 s associated with either a decrease in oxygen saturation by 3% or inducing an Electroencephalographic (EEG) arousal for at least 3 s.

Rhinomanometry

Bilateral nasal resistance curves were measured using anterior rhinomanometry (NR-6 Research, GM Instruments). Three measurements of four breaths with at least a 150 Pa pressure drop were acquired [13]. Average Rohrer coefficients for each nasal passage were used to calculate nasal resistance and air pressure in the choanae at peak inspiratory flow.

Morphological evaluation

During the CBCT (i-CAT; Hatfield, PA, USA) examination, subjects were seated in a chair with his or her Frankfort

Table 1. Comparisons of PSG Parameters, intermaxillary molar width, nasal width, pharyngeal airway volume, intraoral airway volume and nasal airway model resistance before DOME and after DOME

	Before DOME				After DOME				Treatment change				P
	Mean	SD	95% CI		Mean	SD	95% CI		Mean	SD	95% CI		
AHI (events/hr)	17.81	17.56	9.59	26.02	7.82	7.11	4.49	11.14	− 9.99	13.65	− 16.38	− 3.60	< 0.001
ODI (events/hr)	9.67	15.84	2.25	17.08	4.92	5.88	2.16	7.67	− 4.75	11.91	− 10.32	0.82	0.011
AI (events/hr)	5.30	17.53	− 2.91	13.50	0.78	2.34	− 0.32	1.87	− 4.52	15.20	− 11.64	2.60	0.012
LOS (%)	88.15	7.21	84.78	91.52	90.90	4.23	88.92	92.88	2.75	5.53	0.16	5.34	0.036
Intermaxillary molar width (mm)	34.97	3.53	33.32	36.63	42.24	3.28	40.70	43.78	7.27	2.45	6.12	8.41	< 0.001
Nasal width (mm)	22.41	2.34	21.31	23.51	26.68	2.33	25.59	27.77	4.27	1.46	3.59	4.96	< 0.001
Pharyngeal airway volume (cm^3)	16.00	5.57	13.39	18.60	18.20	6.19	15.30	21.10	2.21	3.50	0.57	3.84	0.011
Intraoral airway volume (cm^3)	2.41	4.54	0.29	4.53	1.08	3.08	− 0.36	2.52	− 1.33	2.64	− 2.57	− 0.09	0.036
Nasal airway model resistance ($Pa/cm^3/s$)	0.53	0.38	0.35	0.71	0.16	0.10	0.12	0.21	− 0.37	0.35	− 0.53	− 0.20	< 0.001

DOME, distraction osteogenesis maxillary expansion; AHI, apnea-hypopnea index; ODI, oxygen desaturation index; AI, apnea index; LOS, lowest oxygen saturation; 95% CI, 95% confidential interval

Table 2 Treatment change of pharyngeal airway measurement and correlation between pharyngeal airway measurement and sleep data parameters

							AHI		ODI		AI		LOS	
			Mean	SD	95% CI	P	r_s	P	r_s	P	r_s	P	r_s	P
Depth (mm)	RA	Before DOME	10.44	2.86	9.10 11.77		− 0.354	0.126	− 0.163	0.491	− 0.086	0.720	− 0.051	0.830
		After DOME	10.25	3.07	8.81 11.69		− 0.033	0.890	− 0.386	0.092	0.016	0.946	0.109	0.648
		Treatment change	0.19	2.27	− 0.88 1.25	0.719	− 0.125	0.599	− 0.222	0.346	− 0.150	0.527	− 0.424	0.063
	OA	Before DOME	10.66	2.83	9.34 11.98		− 0.008	0.972	0.241	0.306	− 0.055	0.819	− 0.015	0.948
		After DOME	11.09	2.76	9.80 12.38		0.158	0.506	− 0.063	0.793	0.220	0.351	− 0.044	0.852
		Treatment change	− 0.43	1.91	-1.32 0.46	0.327	0.184	0.437	0.029	0.904	− 0.222	0.347	− 0.317	0.174
	HA	Before DOME	11.75	3.38	10.16 13.33		− 0.038	0.872	0.169	0.475	− 0.172	0.469	− 0.008	0.972
		After DOME	12.71	3.76	10.95 14.46		0.036	0.881	0.069	0.774	-0.031	0.897	0.079	0.740
		Treatment change	− 0.96	2.11	− 1.95 0.03	0.056	0.278	0.235	0.379	0.099	− 0.220	0.352	− 0.159	0.503
Width (mm)	RA	Before DOME	28.35	6.97	24.77 31.30		− 0.443	0.050	− 0.449	0.047*	− 0.138	0.562	− 0.125	0.601
		After DOME	30.16	7.29	26.75 33.57		− 0.234	0.320	− 0.271	0.247	0.214	0.364	0.012	0.961
		Treatment change	− 2.13	7.66	− 5.71 1.46	0.231	− 0.379	0.100	− 0.299	0.201	0.092	0.701	− 0.235	0.318
	OA	Before DOME	26.21	5.75	23.52 28.90		− 0.149	0.531	− 0.140	0.556	0.272	0.245	0.212	0.370
		After DOME	28.04	5.89	25.28 30.80		− 0.249	0.289	− 0.298	0.202	0.145	0.542	0.029	0.905
		Treatment change	− 1.83	4.02	− 3.71 0.05	0.056	0.022	0.927	− 0.113	0.635	− 0.181	0.445	− 0.223	0.344
	HA	Before DOME	28.13	3.95	26.28 29.98		− 0.266	0.258	− 0.340	0.143	− 0.025	0.918	− 0.111	0.642
		After DOME	29.26	3.93	27.42 31.10		− 0.086	0.718	0.000	1.000	0.078	0.743	0.320	0.169
		Treatment change	− 1.13	3.83	− 2.92 0.66	0.202	0.204	0.388	0.071	0.765	0.105	0.658	− 0.007	0.976
Pharyngeal airway volume (cm^3)		Before DOME	16.00	5.57	13.39 18.60		− 0.486	0.030*	− 0.146	0.539	− 0.222	0.347	− 0.122	0.609
		After DOME	18.20	6.19	15.30 21.10		− 0.170	0.473	− 0.151	0.526	0.238	0.311	0.256	0.276
		Treatment change	2.12	3.50	0.57 3.84	0.011	0.027	0.909	− 0.475	0.034*	0.047	0.844	0.187	0.431
Intraoral airway volume (cm^3)		Before DOME	2.41	4.54	0.29 4.53		− 0.303	0.194	− 0.391	0.088	− 0.123	0.607	− 0.548	0.012*
		After DOME	1.08	3.08	− 0.36 2.52		0.097	0.684	0.053	0.825	0.071	0.765	0.374	0.104
		Treatment change	− 1.33	2.64	− 2.57 − 0.09	0.036	− 0.461	0.041*	− 0.478	0.033*	0.561*	0.010	0.218	0.356

DOME, distraction osteogenesis maxillary expansion; RA, retropalatal airway; OA, oropharyngeal airway; HA, hypopharyngeal airway; 95% CI, 95% confidential interval

*Statistically significant at $p < 0.05$

**Statistically significant at $p < 0.001$

Table 3 Treatment change of upper airway ventilation condition before and after DOME

	NA				RA				OA				HA				Site difference	Host hoc
	Mean	SD	95% CI		Mean	SD	95% CI		Mean	SD	95% CI		Mean	SD	95% CI			
Velocity (m/s)																		
Before DOME	15.59	7.29	12.18	19.00	2.71	2.18	1.69	3.73	2.34	1.08	1.83	2.84	2.10	0.89	1.68	2.51	< 0.001	1,2,3
After DOME	7.41	2.08	6.44	8.38	1.76	0.84	1.36	2.15	1.82	0.85	1.42	2.21	1.88	1.02	1.40	2.35	< 0.001	1,2,3
Treatment change	8.18	6.90	4.95	11.41	0.96	1.66	0.18	1.73	0.52	0.61	0.23	0.81	0.22	1.06	− 0.27	0.71	< 0.001	1,2,3
p	< 0.001				0.010				0.003				0.226					
Pressure (Pa)																		
Before DOME	− 158.4	115.3	-212.4	-104.4	-174.8	119.9	-230.9	-118.7	-177.0	118.4	− 232.4	− 121.6	-177.9	117.9	-233.0	-122.7	< 0.001	
After DOME	− 48.6	28.7	− 62.0	− 35.2	− 52.5	31.3	− 67.1	− 37.8	− 54.9	31.8	− 69.8	− 40.1	− 56.9	32.1	− 71.9	− 41.8	< 0.001	
Treatment change	− 109.8	106.1	-159.5	− 60.1	-122.4	110.9	-174.2	− 70.5	-122.1	109.0	− 173.1	− 71.1	-121.0	104.5	-169.9	− 72.1	0.001	
p	< 0.001				< 0.001				< 0.001				< 0.001					

DOME, distraction osteogenesis maxillary expansion; NA, nasal airway; RA, retropalatal airway; OA, oropharyngeal airway; HA, hypopharyngeal airway; a, Significant group differences based on Freidman test with Bonferroni's correction: 1, nasal airway vs RA; 2, nasal airway vs OA; 3, nasal airway vs HA; 95% CI, 95% confidential interval

horizontal plane parallel to the floor, and were instructed to maintain head position, not swallow, and remain in centric occlusion with relaxed tongue and lip positions at the end of expiration. Volume-rendering software (INTAGE Volume Editor; Cybernet, Tokyo, Japan) was used to create the three-dimensional (3D) images manually to allow measurements of the intermaxillary molar widths, nasal width, pharyngeal airway cross-section, and airway volume (Fig. 1). Pharyngeal airway cross-sectional measurements [14] included depth (anteroposterior direction) and width (left-right direction). The pharyngeal and intraoral airway volumes were measured between the palatal plane and the base of epiglottis plane, and the palate and tongue, respectively [15].

Modeling nasal airway ventilation (Fig. 2A, B, C)

The 3D nasal airway was generated from the CBCT data by volume-rendering software (INTAGE Volume Editor; Cybernet Systems, Tokyo, Japan) [15]. The airway was segmented primarily on the basis of image intensity with the threshold set midway between the soft tissue and clear airway value. Subsequently, using mesh-morphing software (DEP Mesh Works/Morpher; IDAJ, Kobe, Japan), the 3D model was converted to a smoothed model without losing the patient-specific pattern of the airway shape. The models were exported to CFD software (Phoenics; CHAM Japan, Tokyo, Japan) in stereo lithographic format. CFD of the nasal airway models was analyzed under the following conditions: (1) the volume of air was flowing at a velocity of 300 cm^3/s, (2) the wall surface was not slippery, and (3) the simulations were repeated 1000 times to calculate mean values. The simulation estimated airflow pressure, where air flowed from the choanae horizontally and was exhaled through both external nares. The nasal airway resistance model was then conformed to nasal rhinomanometry and calculated from air mass flow with the difference in pressure between external nares and choanae according to Ohm's law [15]. We standardized the threshold of the nasal airway model such that nasal airway resistance obtained from CFD corresponded to rhinomanometry nasal airway resistance.

Modeling upper pharyngeal airway ventilation (Fig. 2D, E, F)

We conducted an inspiration simulation (airflow perpendicular to the lower pharyngeal plane at the velocity of 300 cm^3/s) similar to what is described for the nasal airway [11]. We estimated maximal negative pressure and maximum velocity in the nasal, retropalatal, oropharyngeal, and hypopharyngeal segments of the upper airway.

Table 4. Correlation between sleep data and upper airway ventilation condition before DOME, after DOME, and treatment change

		Pre DOME				Post DOME				Treatment change			
		AHI	ODI	AI	LOS	AHI	ODI	AI	LOS	AHI	ODI	AI	LOS
Nasal velocity (m/s)	r_s	0.665	0.416	0.496	− 0.336	0.373	0.333	0.525	− 0.355	0.479	0.661	0.284	− 0.368
	p	0.001**	0.068	0.026*	0.147	0.105	0.152	0.017*	0.125	0.033*	0.002**	0.225	0.110
Nasal pressure (Pa)	r_s	− 0.573	− 0.371	− 0.413	0.380	− 0.452	− 0.417	− 0.443	0.431	− 0.437	− 0.635	− 0.478	0.428
	p	0.008**	0.108	0.071	0.098	0.045*	0.067	0.050	0.058	0.054	0.003**	0.033*	0.060
RA velocity (m/s)	r_s	0.570	0.330	0.195	− 0.140	− 0.019	0.081	− 0.031	− 0.073	0.360	0.308	0.420	0.048
	p	0.009**	0.155	0.411	0.555	0.936	0.734	0.898	0.760	0.119	0.187	0.065	0.840
RA pressure (Pa)	r_s	− 0.700	− 0.519	− 0.440	0.429	− 0.501	− 0.482	− 0.454	0.499	− 0.465	− 0.725	− 0.440	0.506
	p	0.001**	0.019*	0.052	0.059	0.024*	0.031*	0.045*	0.025*	0.039*	0.000**	0.052	0.023*
OA velocity (m/s)	r_s	0.485	0.340	0.093	− 0.372	0.216	0.020	0.012	0.067	0.365	0.423	0.368	− 0.360
	p	0.030*	0.142	0.696	0.107	0.361	0.934	0.959	0.778	0.114	0.063	0.110	0.119
OA pressure (Pa)	r_s	− 0.678	− 0.498	− 0.412	0.398	− 0.533	− 0.515	− 0.466	0.514	− 0.425	− 0.688	− 0.370	0.511
	p	0.001**	0.025*	0.071	0.082	0.015*	0.020*	0.038*	0.020*	0.062	0.001**	0.109	0.021*
HA velocity (m/s)	r_s	0.313	0.146	− 0.060	− 0.176	0.370	0.146	0.178	− 0.080	− 0.158	− 0.265	− 0.121	− 0.204
	p	0.178	0.540	0.800	0.458	0.108	0.538	0.453	0.737	0.505	0.259	0.612	0.389
HA pressure (Pa)	r_s	− 0.714	− 0.510	− 0.459	0.400	− 0.594	− 0.568	− 0.581	0.556	− 0.419	− 0.638	− 0.376	0.491
	p	0.001**	0.022*	0.042*	0.081	0.006**	0.009**	0.007**	0.011*	0.066	0.002**	0.102	0.028*
Nasal width (mm)	r_s	− 0.126	0.025	− 0.064	− 0.126	− 0.179	− 0.192	− 0.206	− 0.008	− 0.399	− 0.091	− 0.099	− 0.041
	p	0.597	0.916	0.787	0.595	0.450	0.418	0.384	0.972	0.082	0.702	0.677	0.864
Intermaxillary first molar width (mm)	r_s	0.072	0.179	− 0.216	− 0.383	0.035	0.042	− 0.218	− 0.158	− 0.002	0.100	− 0.005	− 0.368
	p	0.762	0.450	0.360	0.095	0.885	0.859	0.356	0.506	0.995	0.674	0.983	0.110

DOME, distraction osteogenesis maxillary expansion; RA, retropalatal airway; OA, oropharyngeal airway; HA, hypopharyngeal airway; AHI, apnea-hypopnea index; ODI, oxygen desaturation index; AI, apnea index; LOS, lowest oxygen saturation

**Statistically significant at $p < 0.001$

*Statistically significant at $p < 0.05$

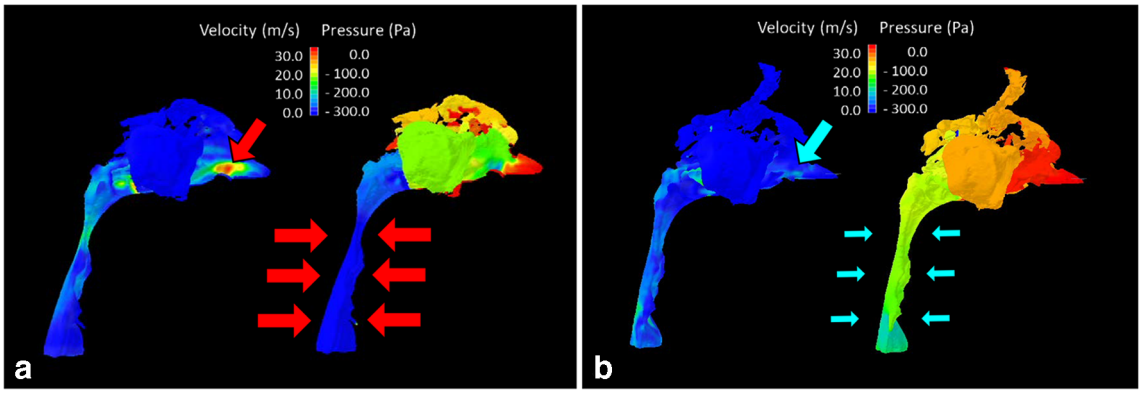

Fig. 3 Improvement of the upper airway ventilation condition upon inspiration using distraction osteogenesis maxillary expansion in an obstructive sleep apnea patient. **A**, before DOME, the nasal airway velocity was high (yellow arrow), and the site was considered an OSA causative site. A large negative pressure was observed at the lower part in the upper airway (red arrow) of the site. The large negative pressure in pharyngeal airway was considered easy to collapse during sleep. **B**, after DOME, the nasal airway velocity slowed (blue arrow), the cause site was improved, and large negative pressure in the pharyngeal airway was reduced (blue arrow). The pharyngeal airway had less negative pressure at inspiration, and became harder to collapse during sleep. Abbreviations: DOME, distraction osteogenesis maxillary expansion; OSA, obstructive sleep apnea

Statistical analysis

Continuous data were presented as means ± standard deviation (SD). Paired *t* tests were conducted to test for significant treatment changes before and after DOME for all study variables. For variables with a non-normal distribution or differing variances, significant treatment changes were determined using the nonparametric Wilcoxon rank test. Intersite differences were determined using the Friedman test with Bonferroni correction. Spearman's correlation coefficients were calculated to evaluate the relationships between morphological and ventilation parameters and PSG outcome. Statistical significance was defined as $p < 0.05$. Statistical analyses were conducted using SPSS Ver 24.

Results

Of the 20 subjects enrolled (five females and 15 males), the mean (± SD) age was 29.6 ± 8.3 years. Average height was 176.7 ± 8.5 cm, average weight was 79.7 ± 20.1 kg, and average BMI was 25.8 ± 6.2 kg/m^2.

Polysomnography

Mean AHI improved from 17.81 ± 17.56 to 7.82 ± 7.11 events per hour ($p < 0.001$). Mean lowest oxygen saturation improved from 88.15 ± 7.21 to 90.90 ± 4.23% ($p < 0.05$). (Table 1). Oxygen desaturation index (ODI) and Apnea index (AI) decreased from 9.7 ± 16 events per hour to 4.9 ± 6 events per hour; and from 5.3 ± 18 events per hour to 0.78 ± 2 events per hour, respectively ($p < 0.001$).

Morphologic measurements

Intermaxillary molar width increased from 34.04 ± 3.54 to 41.6 ± 3.1 mm ($p < 0.001$, Table 1) after DOME. The nasal floor width at the level of internal nasal valve increased from 21.0 ± 2.1 to 26.2 ± 2.3 mm ($p < 0.001$) after DOME.

Pharyngeal airway size

No significant difference in width or depth of the pharyngeal airway was found after treatment (Table 2). The pharyngeal airway volume after DOME was significantly greater (Table 1).

Rhinomanometry-based computational fluid dynamic modeling (Fig. 2D, E, F)

Nasal airway resistance after DOME (0.48 ± 0.20 Pa/cm^3/s) was significantly lower compared to baseline (0.65 ± 0.2 Pa/cm^3/s, $p < 0.001$). The velocity of nasal airflow after DOME (7.41 ± 2.08 m/s) was significantly lower than baseline (15.59 ± 7.29 m/s, $p < 0.001$, Table 3). The velocity of the retropharyngeal, oropharyngeal, and hypopharyngeal airflow after DOME decreased significantly. Reduction of airflow velocity in the nasal passage was significantly greater than the pharynx.

Correlations with polysomnography

AHI was positively correlated with nasal airflow velocity, and was negatively correlated with the nasal, retropalatal, oropharyngeal, and hypopharyngeal airway pressure. The apnea index (AI) had a similar tendency as the AHI (Table 4). The

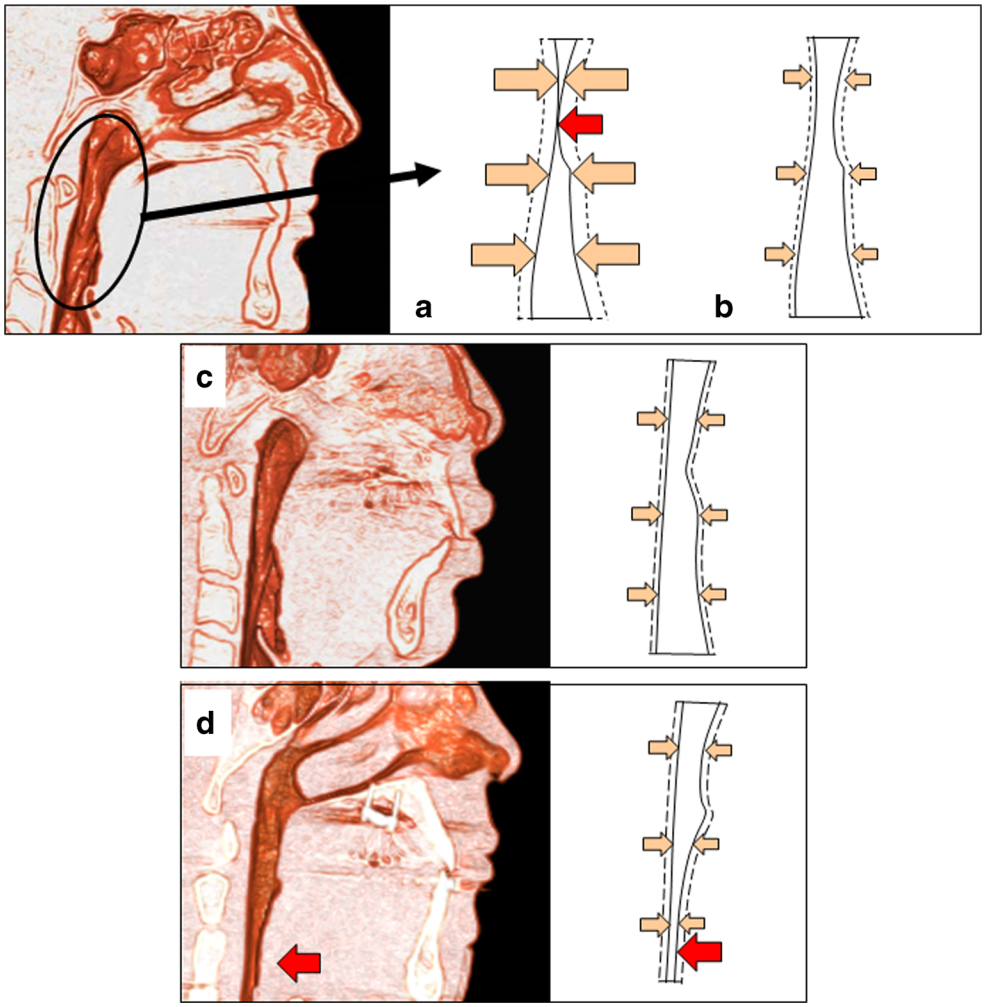

Fig. 4 The schematic diagram of effect of distraction osteogenesis maxillary expansion on the negative pressure in the pharyngeal airway and the responder and non-responder subjects of distraction osteogenesis maxillary expansion. **A**, Before DOME, the pharyngeal airway collapses (red arrow) as a result of negative pharyngeal airway pressure (large orange arrow) during inspiration). Dotted line, before inspiration; solid line, during inspiration. **B**, After DOME, there is a reduction of pharynx airway negative pressure during inspiration (small orange arrow), and less collapsibility of the pharyngeal airway. The pharyngeal airway remains patent during inspiration. Dotted line, before inspiration; solid line, during inspiration. C, C, After DOME, responder, initial pharyngeal airway had adequate width (RA 11.7 mm, OA 14.9 mm, HA 18.9 mm) and small negative pressure (− 108 Pa). Therefore, the airway remains patent and responded to DOME intervention. **D**, After DOME, non-responder, because hypopharyngeal airway width (red arrow; RA 11.0 mm, OA 7.5 mm, HA 7.2 mm) was narrow, airway remains collapsible despite small negative pressure (− 151 Pa) after DOME intervention

intermaxillary first molar width, nasal floor width, and pharyngeal airway and intraoral volumes show modest negative correlations with AHI and ODI.

Discussion

Distraction osteogenesis maxillary expansion (DOME) is a reliable method to expand nasal floor width and hard palatal vault in adults with obstructive sleep apnea (OSA). DOME results in a reduction in the apnea-hypopnea index (AHI) and subjective report of improved nasal breathing [16]. Using rhinomanometry and computational fluid dynamic (CFD) modeling, we propose a mechanism of how DOME reduces upper airway pharyngeal collapse in adults with OSA. Using both radiographic and physiologic parameters before and after DOME, we examine how maxillary constriction serves as a risk factor for adult OSA. Maxillary constriction is an under-recognized finding among adult patients with OSA. For such patients, surgical-assisted rapid maxillary expansion decrease nasal airway resistance (62.9%) [4]. In our study, nasal flow resistance is reduced from 0.53 to 0.16 Pa/cm^3/s (30.2%). Of the 20 subjects enrolled, the AHI decreased by 44%, while patients reported significant subjective improvement of nasal breathing. There was no correlation found between degree of expansion and improvement as assessed by AHI.

We modeled nasal and upper airway airflow and pressure using CFD. While previous CFD is mostly imaging-based,

ours include physiologic airflow measurements obtained from rhinomanometry. While CFD has limitations in the use of an awake and rigid airway for modeling, our physiologic nasal and oral flow data via rhinomanometry through the nasal and pharyngeal airway significantly improve real-life simulation and approximation.

Based on our findings, we propose the following mechanism of action for maxillary expansion in adults. Prior to DOME, subjects presented with high-flow velocity in the nasal airway. This was significantly reduced after DOME (Fig. 3). Relative to the nasal airway, the pharyngeal airway showed low airflow velocity before and after DOME. While the pharyngeal airway did not show significant changes in airflow velocity after DOME, it did change significantly with regard to negative pressure. Reduction in nasal airflow velocity is associated with reduced negative pressure of the pharyngeal airway (Table 3, Figs. 3 and 4). Concurrently, the reduction of nasal airflow velocity and pharyngeal upper airway negative pressure is associated with improvement of OSA based on AHI, ODI, and lowest oxygen saturation. This hypothesis had been suggested previously with imaging-based CFD [17], but without the physiologic nasal flow measurements which we have addressed with the present study.

Previously, similar types of study without individual-specific nasal airflow measurements suggested that pharyngeal airway volume is the primary determinant of AHI [18–21]. The rationale is that the smaller the upper airway, the higher the AHI. However, this hypothesis does not account for the nasal airflow which impacts collapsibility of the pharyngeal airway. Using subjects as their own controls before and after DOME, we propose that nasal airflow is a primary determinant of upper airway collapsibility. This is actually further corroborated by two cases that failed to show improvement in AHI after DOME. One subject showed persistent nasal obstruction after DOME due to severe septal deviation. The other subject had the smallest pharyngeal airway of the cohort. Therefore, treatment success from maxillary expansion still needs to take into account two major factors: (1) resolution of nasal obstruction and (2) improvement of nasal airflow may be inadequate to overcome pharyngeal airway collapsibility if the airway volume is excessively reduced. We did not find significant direct correlations between amount of expansion and sleep study parameters. The morphological measurements of the facial skeleton alone are insufficient to capture other elements of sleep including loop gain, arousal threshold, and muscle tone.

There are a number of pertinent limitations to our study. The computed tomography data was not obtained during sleep. It is unethical, however, to expose patients to the degree of radiation required to image upper airway movements during sleep. This is why we included physiologic nasal flow measurements to CFD modeling, which does assume rigid airway morphology. The nasal airway value was similar to the biological data and we considered that the value of the pharyngeal airway was similar to the biological data. However, CFD is a mechanical simulation and should be calibrated in practice. The sample size is not small in comparison to similar types of studies, but it is not large enough for us to make stronger clinical inferences. Lastly, while all subjects presented with transverse maxillary hypoplasia, some also present with anterior-posterior hypoplasia of the upper or lower jaw which may lessen the generalizability of our proposed mechanism.

Conclusion

While previous literature mostly acknowledged that a smaller upper pharyngeal airway is correlated with increased OSA risk and severity, we propose the additional importance of nasal airflow. Based on individual-specific CFD modeling that incorporates both airway morphology and air flow measurements, we propose that: (1) reduction of nasal airflow velocity impacts negative pressure of the pharyngeal airway, which contributes to reduction of OSA severity; (2) DOME demonstrates the efficacy of maxillary expansion in adults for the improvement of nasal breathing and OSA severity.

Compliance with ethical standards

Conflict of interest The authors declare that they have no conflict of interest.

Ethical approval This study was approved by the Institutional Review Board of Stanford University (Protocol 36385, IRB 6208) and the ethics committee of the Graduate School of Medical and Dental Sciences of Kagoshima University, Kagoshima, Japan. This study complied with the 1964 Helsinki Declaration and its later amendments.

Informed consent Informed consent was obtained from all individual participants included in the study.

Abbreviations 3D, three-dimensional; AHI, apnea-hypopnea index; AI, apnea index; CFD, computational fluid dynamic; D, depth; DOME, distraction osteogenesis maxillary expansion; EB plane, a plane parallel to the hard plate passing through the base of the epiglottis; HA, hypopharyngeal airway; LOS, lowest oxygen saturation; OA, oropharyngeal airway; ODI, oxygen desaturation index; OSA, obstructive sleep apnea; PL plane, a plane passing through the hard plate; RA, retropalatal airway; W, width

References

1. Guilleminault C, Lee JH, Chan A (2005) Pediatric obstructive sleep apnea syndrome. Arch Pediatr Adolesc Med 159(8):775–785
2. Cistulli PA (1996) Craniofacial abnormalities in obstructive sleep apnoea: implications for treatment. Respirology. 1(3):167–174

3. Pirelli P, Saponara M, Guilleminault C (2004) Rapid maxillary expansion in children with obstructive sleep apnea syndrome. Sleep 27(4):761–766
4. Zambon CE, Ceccheti MM, Utumi ER et al (2012) Orthodontic measurements and nasal respiratory function after surgically assisted rapid maxillary expansion: an acoustic rhinometry and rhinomanometry study. Int J Oral Maxillofac Surg 41(9):1120–1126
5. Villa MP, Rizzoli A, Miano S, Malagola C (2011) Efficacy of rapid maxillary expansion in children with obstructive sleep apnea syndrome: 36 months of follow-up. Sleep Breath 15(2):179–184
6. Vinha PP, Eckeli AL, Faria AC, Xavier SP, de Mello-Filho FV (2015) Effects of surgically assisted rapid maxillary expansion on obstructive sleep apnea and daytime sleepiness. Sleep Breath
7. Vinha PP, Faria AC, Xavier SP, Christino M, de Mello-Filho FV (2015) Enlargement of the pharynx resulting from surgically assisted rapid maxillary expansion. J Oral Maxillofac Surg
8. Liu SY, Guilleminault C, Huon LK, Yoon A (2017) Distraction osteogenesis maxillary expansion (DOME) for adult obstructive sleep apnea patients with high arched palate. Otolaryngol Head Neck Surg Off J Am Acad Otolaryngol Head Neck Surg 157(2):345–348
9. Mosleh MI, Kaddah MA, Abd ElSayed FA, ElSayed HS (2015) Comparison of transverse changes during maxillary expansion with 4-point bone-borne and tooth-borne maxillary expanders. Am J Orthod Dentofac Orthop 148(4):599–607
10. Mihaescu M, Mylavarapu G, Gutmark EJ, Powell NB (2011) Large eddy simulation of the pharyngeal airflow associated with obstructive sleep apnea syndrome at pre and post-surgical treatment. J Biomech 44(12):2221–2228
11. Iwasaki T, Takemoto Y, Inada E et al (2014) The effect of rapid maxillary expansion on pharyngeal airway pressure during inspiration evaluated using computational fluid dynamics. Int J Pediatr Otorhinolaryngol 78(8):1258–1264
12. Liu SY, Huon LK, Iwasaki T et al (2016) Efficacy of maxillomandibular advancement examined with drug-induced sleep endoscopy and computational fluid dynamics airflow modeling. Otolaryngol Head Neck Surg 154(1):189–195
13. Clement PA, Gordts F (2005) Consensus report on acoustic rhinometry and rhinomanometry. Rhinology. 43(3):169–179
14. Iwasaki T, Sato H, Suga H et al (2017) Relationships among nasal resistance, adenoids, tonsils, and tongue posture and maxillofacial form in Class II and Class III children. Am J Orthod Dentofac Orthop 151(5):929–940
15. Iwasaki T, Saitoh I, Takemoto Y et al (2013) Tongue posture improvement and pharyngeal airway enlargement as secondary effects of rapid maxillary expansion: a cone-beam computed tomography study. Am J Orthod Dentofac Orthop 143(2):235–245
16. Abdelwahab M, Yoon A, Okland T, Poomkonsarn S, Gouveia C, Liu SY (2019) Impact of distraction osteogenesis maxillary expansion on the internal nasal valve in obstructive sleep apnea. Otolaryngol Head Neck Surg Off J Am Acad Otolaryngol Head Neck Surg 194599819842808
17. Wootton DM, Luo H, Persak SC et al (2014) Computational fluid dynamics endpoints to characterize obstructive sleep apnea syndrome in children. J Appl Physiol (1985) 116(1):104–112
18. Arens R, Sin S, McDonough JM et al (2005) Changes in upper airway size during tidal breathing in children with obstructive sleep apnea syndrome. Am J Respir Crit Care Med 171(11):1298–1304
19. Liu SY, Huon LK, Lo MT et al (2016) Static craniofacial measurements and dynamic airway collapse patterns associated with severe obstructive sleep apnoea: a sleep MRI study. Clin Otolaryngol 41(6):700–706
20. Huon LK, Liu SY, Shih TT, Chen YJ, Lo MT, Wang PC (2016) Dynamic upper airway collapse observed from sleep MRI: BMI-matched severe and mild OSA patients. Eur Arch Otorhinolaryngol 273(11):4021–4026
21. Van Holsbeke C, Vos W, Van Hoorenbeeck K et al (2013) Functional respiratory imaging as a tool to assess upper airway patency in children with obstructive sleep apnea. Sleep Med 14(5):433–439